AD-A087 961 SOUTHWEST RESEARCH INST SAN ANTONIO TEX F/G 11/6
CRACK TIP PLASTICITY ASSOCIATED WITH CORROSION ASSISTED FATIGUE--ETC(U)
JUL 80 D L DAVIDSON, J LANKFORD N00014-75-C-1038
UNCLASSIFIED SwRI-02-4268 NL

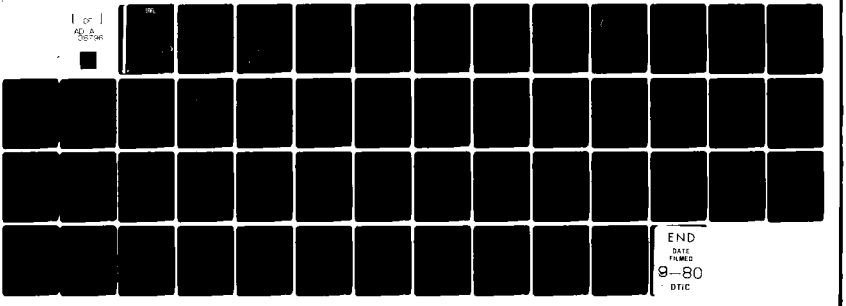

Contract NOOO14-75-C-1038

CRACK TIP PLASTICITY ASSOCIATED WITH CORROSION ASSISTED FATIGUE

D.L. Davidson and J. Lankford
Southwest Research Institute
P. O. Drawer 28510
San Antonio, Texas 78284

Interim Report for Period June 1979 - June 1980

Prepared for

OFFICE OF NAVAL RESEARCH
800 North Quincy Street
Arlington, Virginia 22217

31 JULY 1980

UNCLASSIFIED

SECURITY CLASSIFICATION OF THIS PAGE (When Data Entered)

REPORT DOCUMENTATION PAGE	READ INSTRUCTIONS BEFORE COMPLETING FORM
1. REPORT NUMBER (12) 51 / 2. GOVT ACCESSION NO. AD-A087961	3. RECIPIENT'S CATALOG NUMBER
4. TITLE (and Subtitle) (4) CRACK TIP PLASTICITY ASSOCIATED WITH CORROSION ASSISTED FATIGUE.	5. TYPE OF REPORT & PERIOD COVERED (9) Interim Report - June 1979 – June 1980
(14) SWRI-02-4268	6. PERFORMING ORG. REPORT NUMBER
7. AUTHOR(s) (1) D. L. Davidson J. Lankford	8. CONTRACT OR GRANT NUMBER(s) (15) N00014-75-C-1038
9. PERFORMING ORGANIZATION NAME AND ADDRESS Southwest Research Institute P. O. Drawer 28510 San Antonio, TX 78284	10. PROGRAM ELEMENT, PROJECT, TASK AREA & WORK UNIT NUMBERS NR 036-109/2-25/76(471)
11. CONTROLLING OFFICE NAME AND ADDRESS Office of Naval Research 800 North Quincy Street Arlington, Virginia 22217	12. REPORT DATE 31 May 1980
	13. NUMBER OF PAGES 45 + prelims
14. MONITORING AGENCY NAME & ADDRESS(if different from Controlling Office) (1) 31 Jul 80	15. SECURITY CLASS. (of this report) Unclassified
	15a. DECLASSIFICATION/DOWNGRADING SCHEDULE

16. DISTRIBUTION STATEMENT (of this Report)

Reproduction in whole or in part is permitted for any purpose of the United States Government. Distribution is unlimited.

17. DISTRIBUTION STATEMENT (of the abstract entered in Block 20, if different from Report)

18. SUPPLEMENTARY NOTES

19. KEY WORDS (Continue on reverse side if necessary and identify by block number)

Corrosion fatigue
Crack tip plasticity
Fatigue-environment interaction
Low-carbon steel
Fatigue crack propagation
Crack tip stresses
Crack tip strains

20. ABSTRACT (Continue on reverse side if necessary and identify by block number)

The effects of a water vapor environment on crack tip plasticity in low-carbon steel have been further examined. Strains in the plastic zone, as determined by stereoimaging, have been used to compute stresses at the same locations, and an estimate of the energy expended for creation of new crack area may also be computed using the same strains. These values are compared with similar information derived previously using plastic zone subgrain size distributions as determined by electron channeling.

DD FORM 1 JAN 73 1473 EDITION OF 1 NOV 65 IS OBSOLETE

328200

UNCLASSIFIED

SECURITY CLASSIFICATION OF THIS PAGE (When Data Entered)

There is general agreement between the data determined by the two techniques. A model is offered for including the effects of water vapor upon crack tip plasticity into the damage accumulation analysis of fatigue crack propagation. A critical discussion is also given of the findings to date on the effects of environment on crack tip plasticity, and it is concluded that those findings may be explained by changes in the material properties very close to the crack tip, rather than in the bulk of the plastic zone.

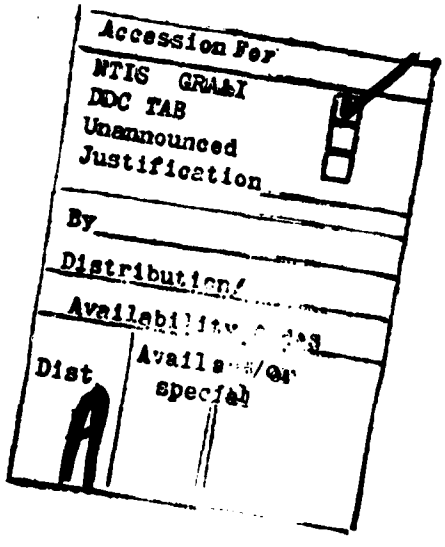

TABLE OF CONTENTS

LIST OF FIGURES

The information on this page is offered to assist in interpreting Figures 1-4.

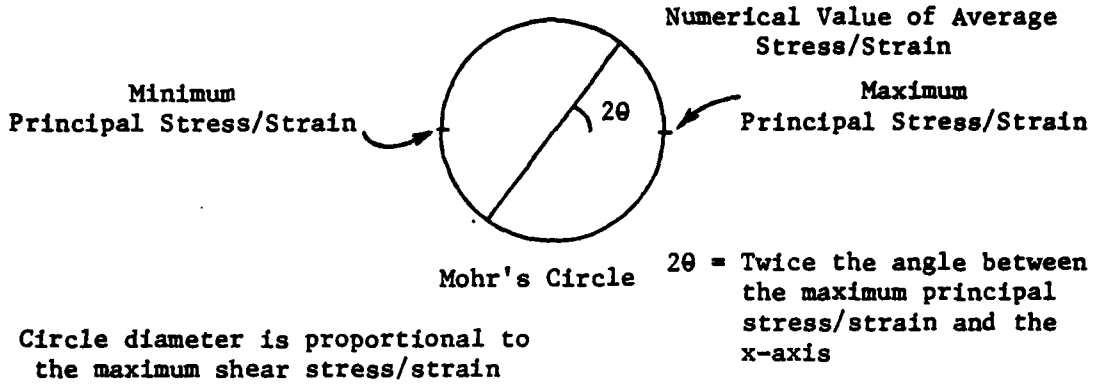

Notes:

1. At some x,y no stress circle is found because the computational procedure for stress did not converge. This occurred principally along boundaries where the strain calculation may be less accurate.

2. Principal stresses are assumed to have the same direction as principal strains.

FATIGUE CRACK TIP STRESS RANGE AND ENERGY CALCULATIONS AS DERIVED FROM STRAINS BY STEREOIMAGING

I. INTRODUCTION

The computation of stresses from the strains measured near fatigue crack tips by stereoimaging has been accomplished. This report outlines the methods used to make these calculations, together with the assumptions implicit in them, and presents the results which have been obtained to date.

Another method has been devised to calculate the energy expended in creation of a unit area of new crack, dW/dA. The plastic strain range, as determined by stereoimaging, is used together with the hysteretic energy loss per cycle to make this calculation. The hysteretic energy loss per cycle has been both directly measured, and also derived, using previously obtained subgrain size information, giving equivalent results.

The information on the effect of water vapor on fatigue crack plasticity which has been determined during this past year and previous years has been used to include both environmental effects and threshold effects into the damage accumulation model for fatigue crack growth. Finally, this report will summarize the effects of water vapor on fatigue crack tip stresses, strains, energies, and opening modes, and will offer some possible mechanistic interpretations of these results.

II. DETERMINATION OF CYCLIC STRESS RANGE

A. Introduction

The cyclic stress range distribution within the fatigue crack tip plastic zone was previously determined[1] using subgrains as small "stress gauges." Because of the successful correlation between strain distribution, as determined from subgrains, with that determined by stereoimaging analysis,[2] it is desirable to determine stress from stereoimaging strain in order to make a similar correlation. Another reason for computation of stresses is to try to determine experimentally the magnitude of the mean stress, or hydrostatic stress, within the plastic zone. This is useful because of the role mean stress is thought to have in environmentally assisted crack propagation.

B. Calculation of Principal Stress

The surface of any specimen is, by definition, in a state of plane stress, which means no constraint exists in the through-thickness direction which can support a stress perpendicular to the specimen surface plane. It is, therefore, not possible to determine stresses in the condition of plane strain, although all evidence collected to date indicates

that the plastic zone sizes and shapes are about what would be expected for the crack tip plastic zone to be in plane strain. Thus, a peculiar set of conditions pertains: the material constraints are such that the crack tip plasticity is indicative of conditions within the specimen, so that the through-thickness variations are minor, while the stresses must be considered as though the specimen itself is wholly in a state of plane stress. The significance of these factors and their exact meaning are still being pondered. However, our tentative conclusion is that for most of the plastic zone, the stresses as well as strains, reflect conditions on the interior of the specimen as well as on the surface; which is to say that for the constrained plasticity conditions used here, the computed stresses are, more-or-less, those which would be found in the specimen interior, although immediately at the crack tip, this situation has a larger degree of uncertainty.

The strains measured by stereoimaging are considered to be total strains; thus $\Delta\Gamma_i$, the measured principal strain range, is

$$\Delta\Gamma_i = \Delta\varepsilon_i + \Delta e_i \qquad (1)$$

where $\Delta\varepsilon_i$ = the plastic strain range and Δe_i = the elastic strain range. With several assumptions, Appendix A, it is possible to separate elastic and plastic strain range, and, through the use of the cyclic stress-strain curve, to compute the magnitude of the principal stress ranges from the principal strain ranges. It is also assumed that the principal stresses have the same direction as the principal strains.

Computations of the stresses for specimens cycled in the wet and dry environments are shown in Figures 1 and 2. These are Mohr's circle diagrams of stress, which match the Mohr's circle diagrams of strain, shown in Figures 3 and 4 (reprinted from last year's report). The angular variation in effective stress range, $\Delta\sigma_{eff}$, is shown for each environment in Figures 5 and 6 (see Eq. A7 in Appendix A for definition of $\Delta\sigma_{eff}$). Also shown on these figures is the angular variation in stress range computed from subgrain formation. There is remarkable agreement, Table 1, in the maximum value of stress at the crack tip as determined by the two different methods, for both environments, even though there are differences in the angular distributions of stress. These differences have not yet been resolved, but they may stem from changes in the plane stress-plane strain mix measured by the two techniques. (Stereoimaging must be done on the specimen surface, while the subgrain data is best taken from the near subsurface region; a depth from the surface of 0.1 mm was used in previous work.) The data in Figs. 5 and 6 also indicate that the distribution function for stresses computed from stereoimaged strains may not be the same as that derived from subgrain data. This situation is still being explored.

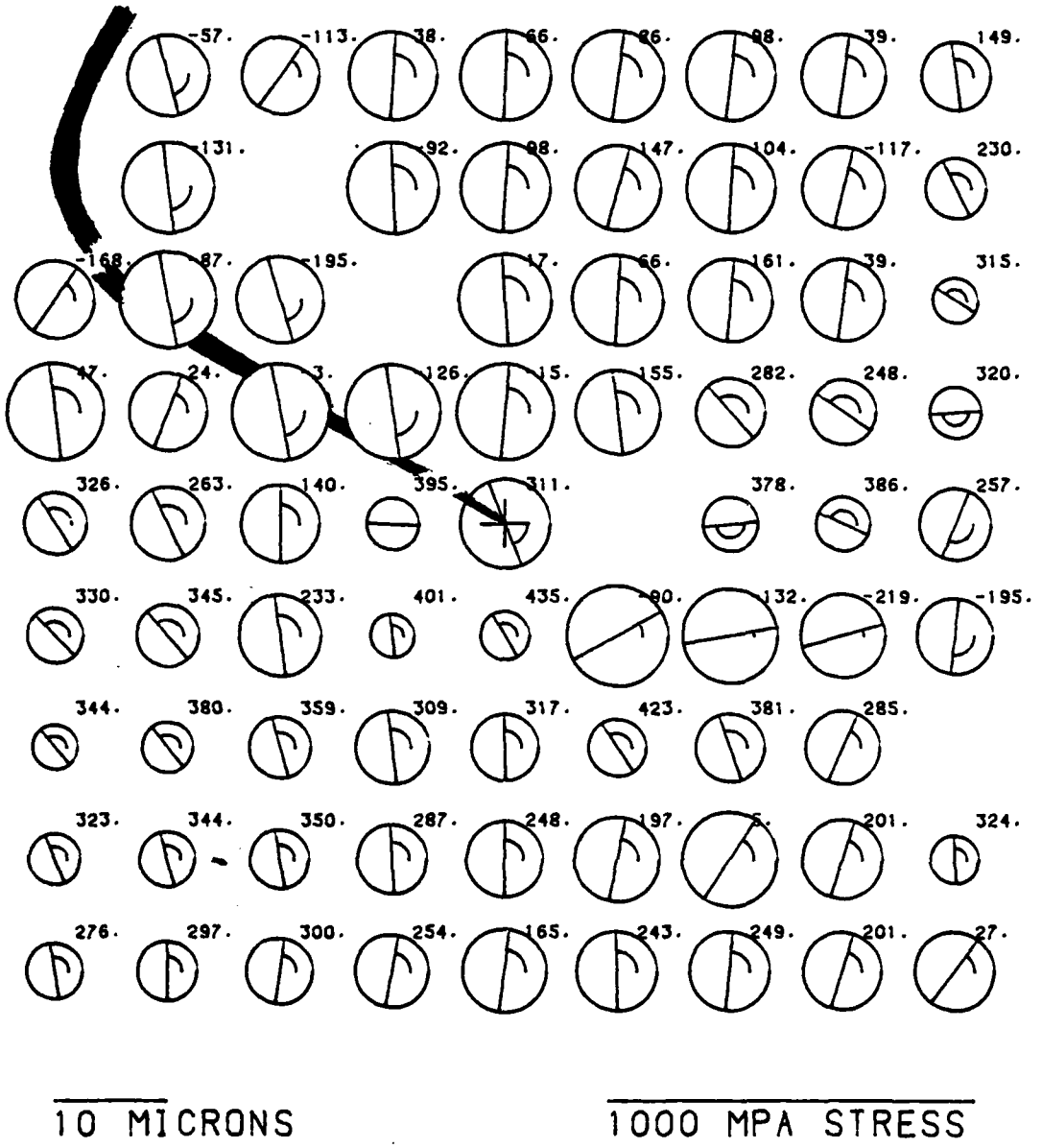

Figure 1a. Mohr's circles of stress, course grid. Average stress is given as the number. Dry nitrogen environment, $\Delta K = 11\ MN/m^{3/2}$.

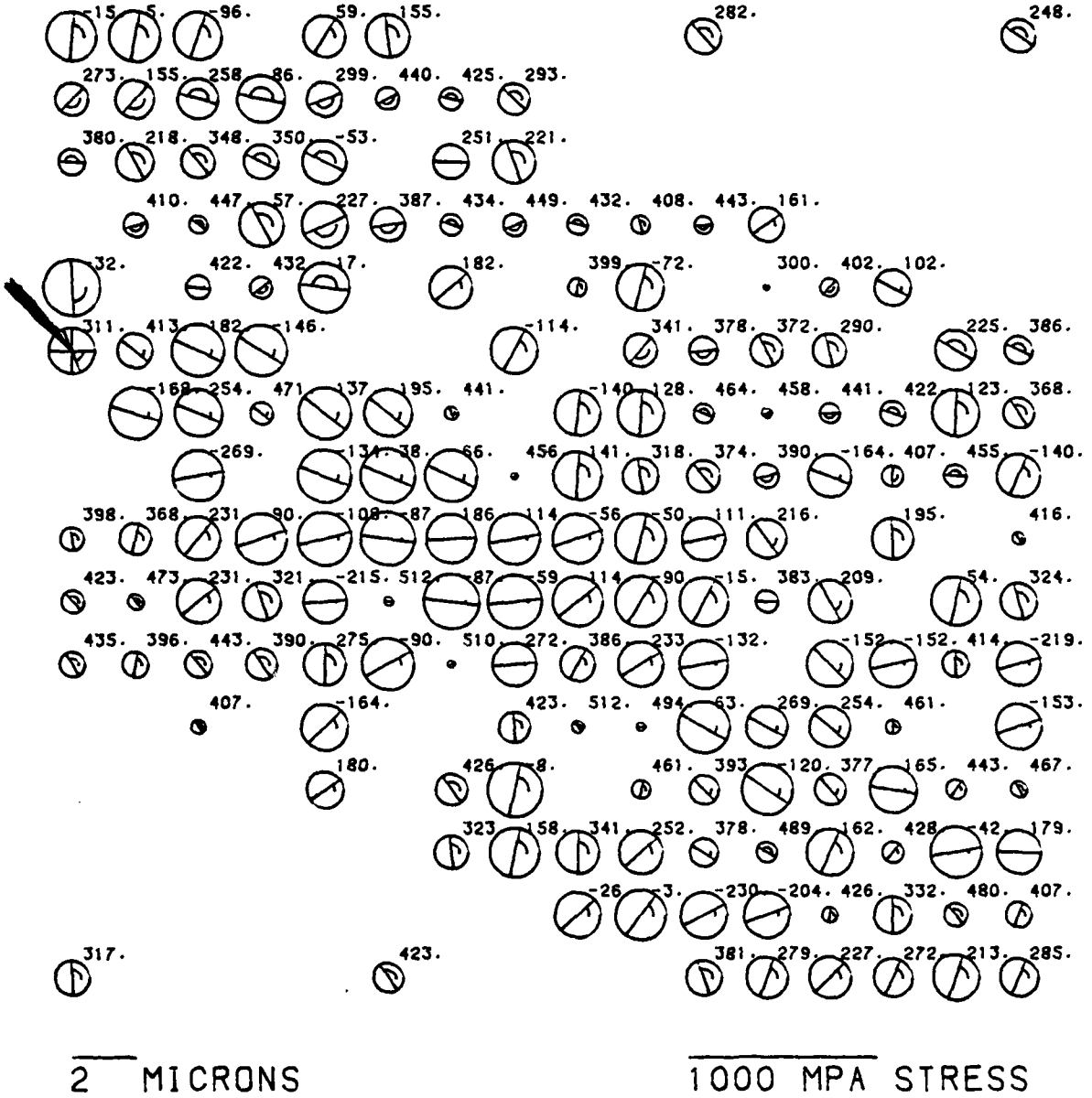

Figure 1b. Mohr's circles of <u>stress</u>, fine grid, dry nitrogen environment, $\Delta K = 11\ MN/m^{3/2}$.

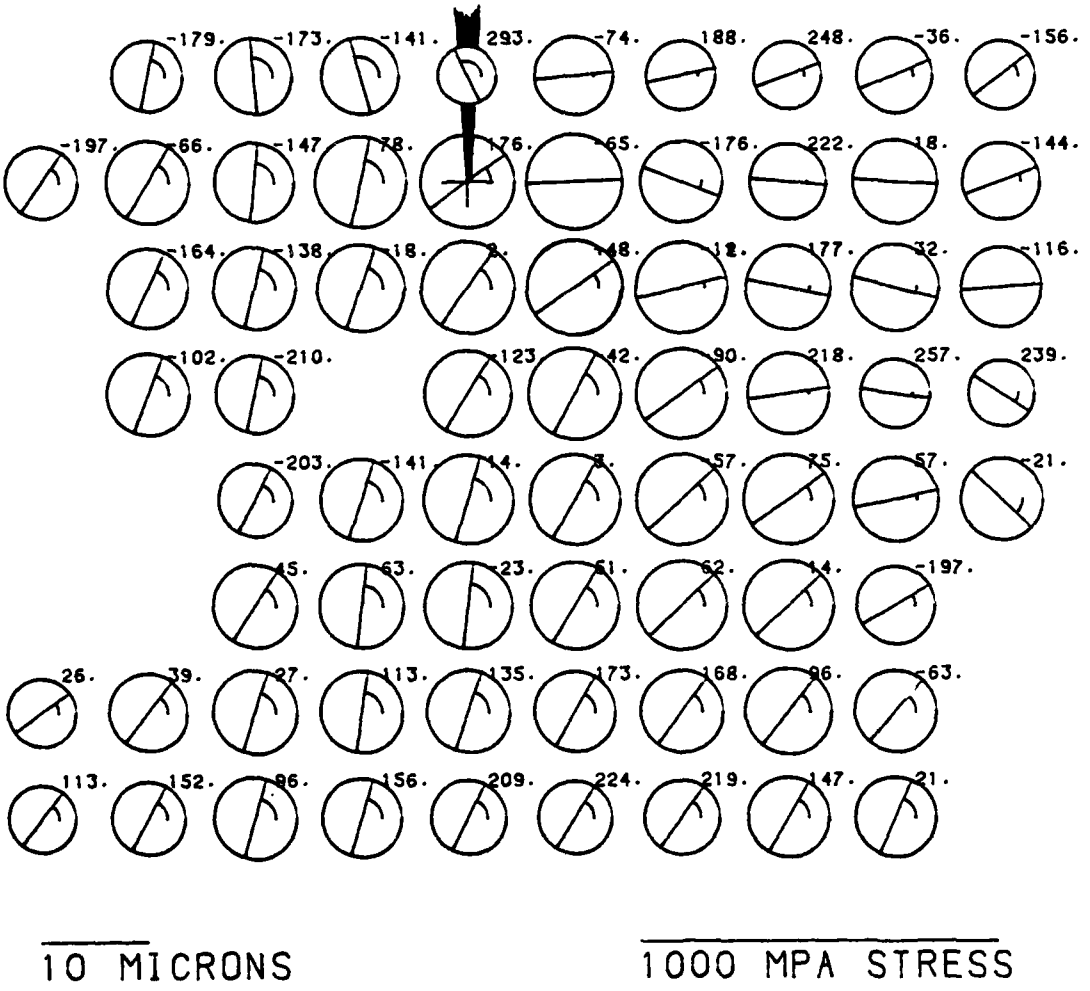

Figure 2a. Mohr's circles of <u>stress</u>, course grid, wet air environment, $\Delta K = 11\ MN/m^{3/2}$.

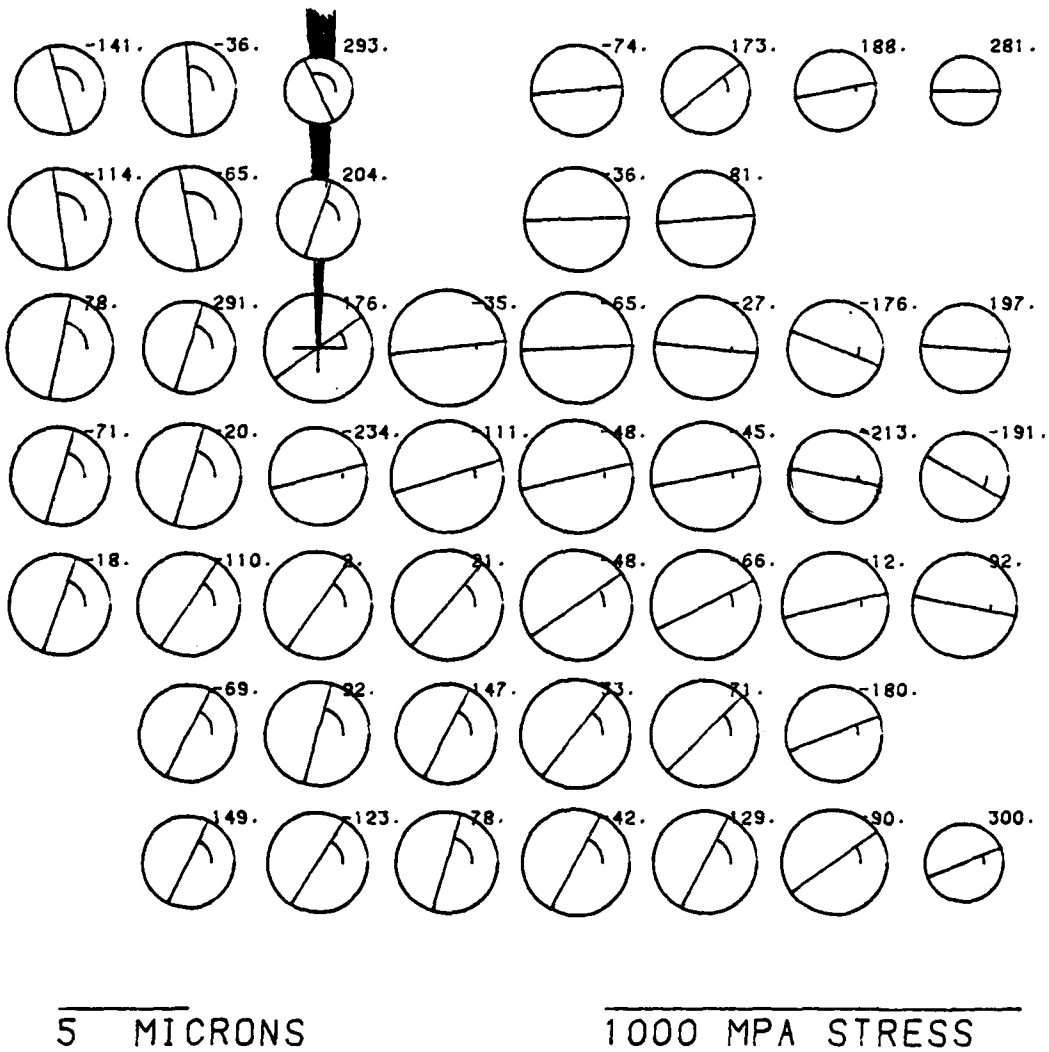

Figure 2b. Mohr's circles of <u>stress</u>, fine grid, wet air environment, $\Delta K = 11\ MN/m^{3/2}$.

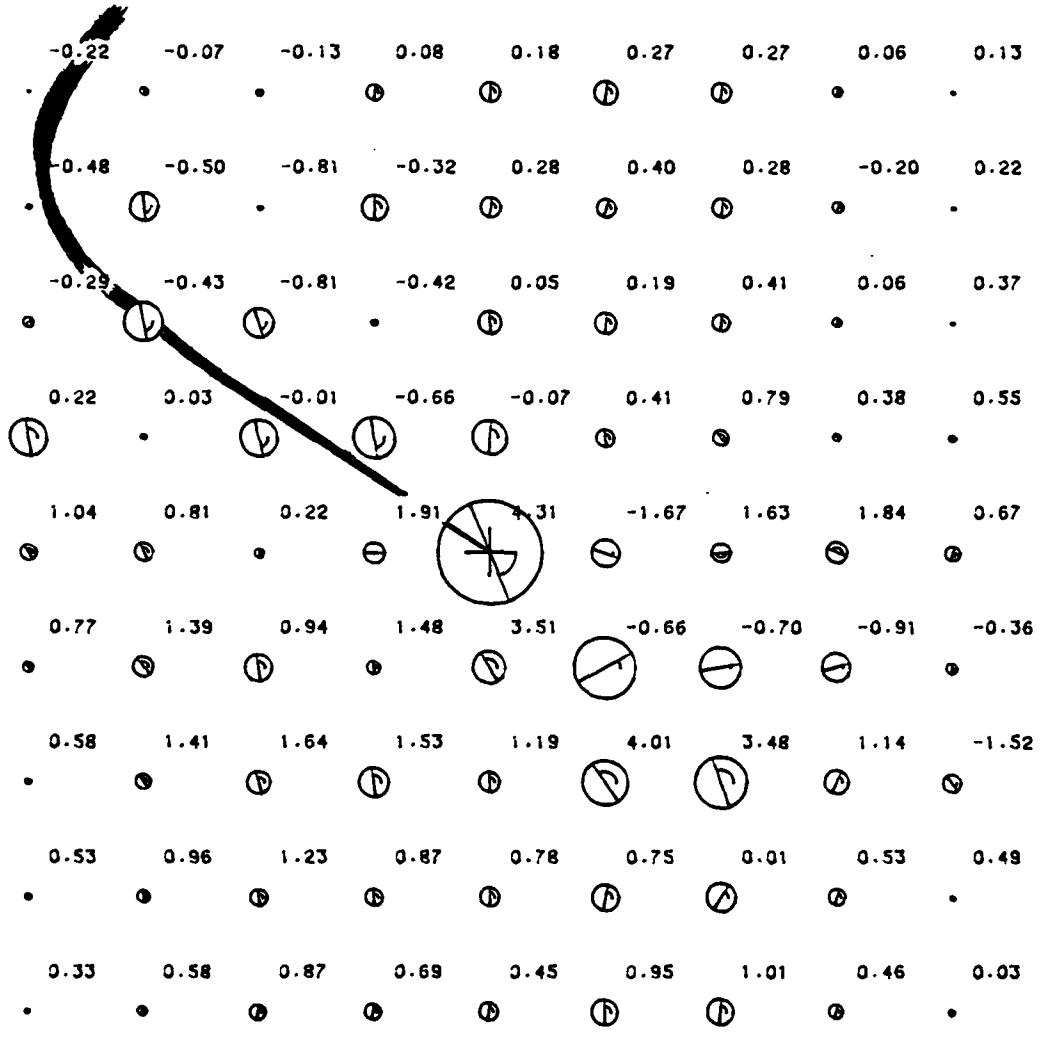

Figure 3a. Mohr's circles of <u>strain</u>, course grid, dry nitrogen environment, $\Delta K = 11\ MN/m^{3/2}$.

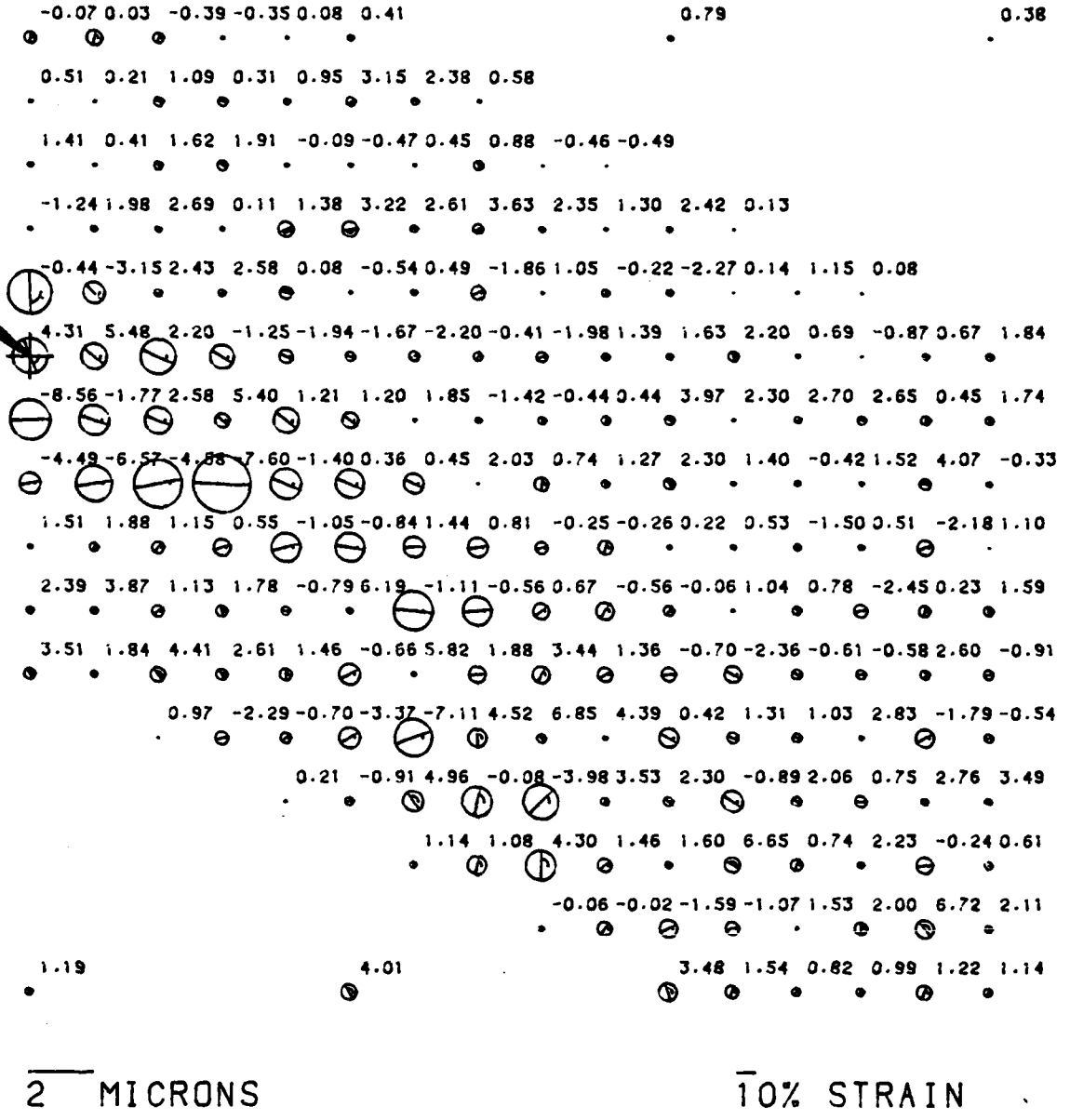

Figure 3b. Mohr's circles of strain, fine grid, dry nitrogen environment, $\Delta K = 11$ MN/m$^{3/2}$.

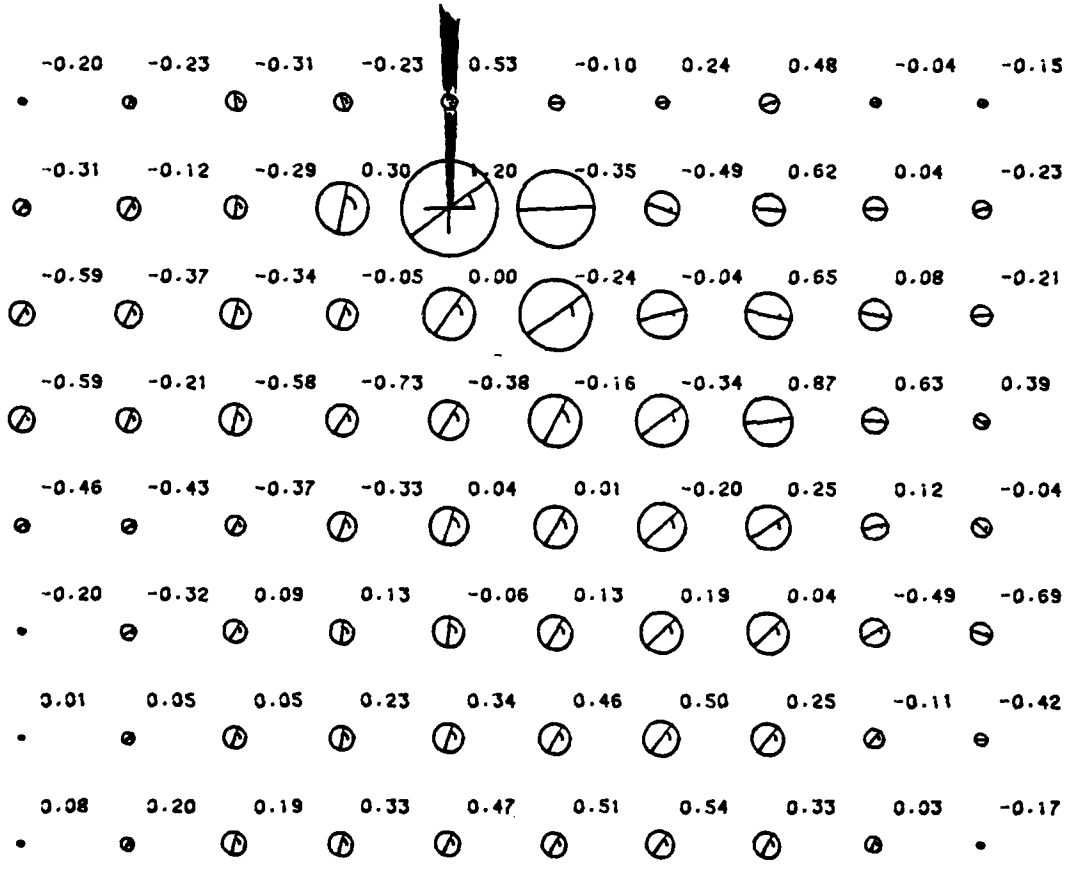

Figure 4a. Mohr's circles of <u>strain</u>, course grid, wet air environment, $\Delta K = 11\ MN/m^{3/2}$.

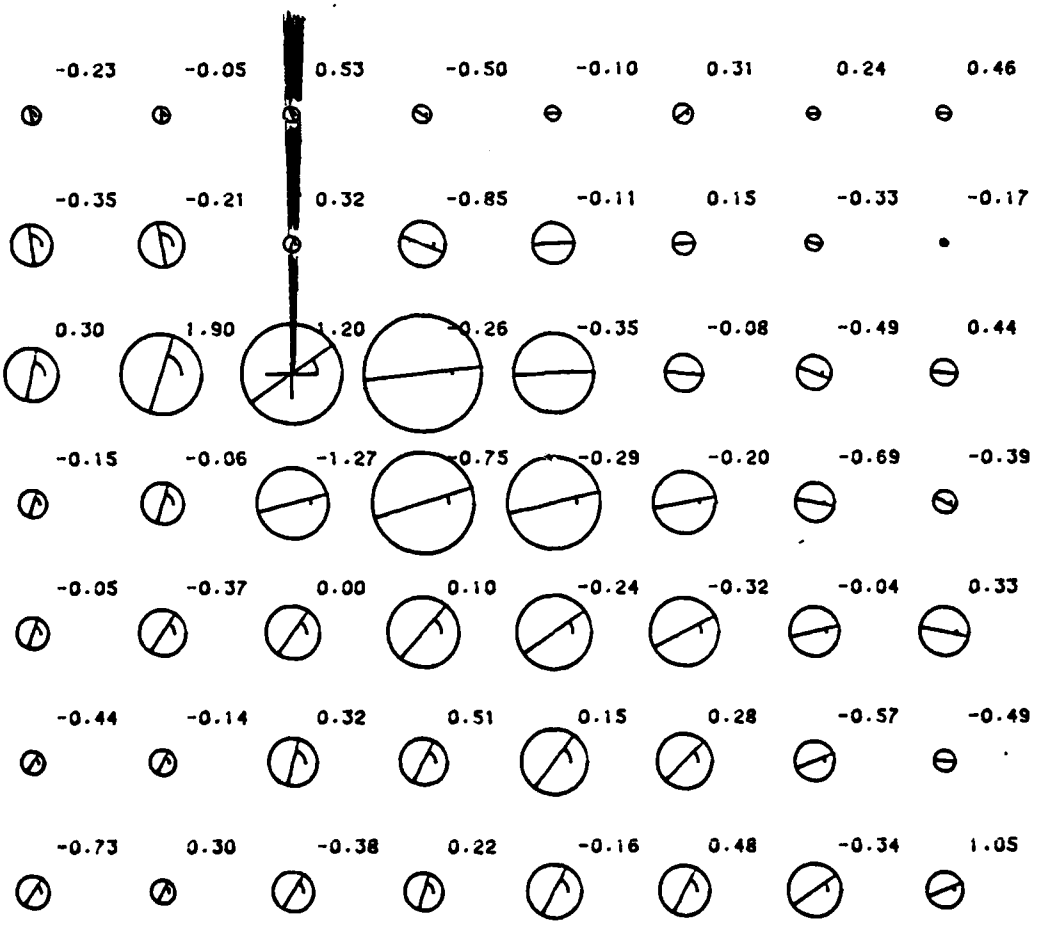

Figure 4b. Mohr's circles of <u>strain</u>, fine grid, wet air environment, $\Delta K = 11\ MN/m^{3/2}$.

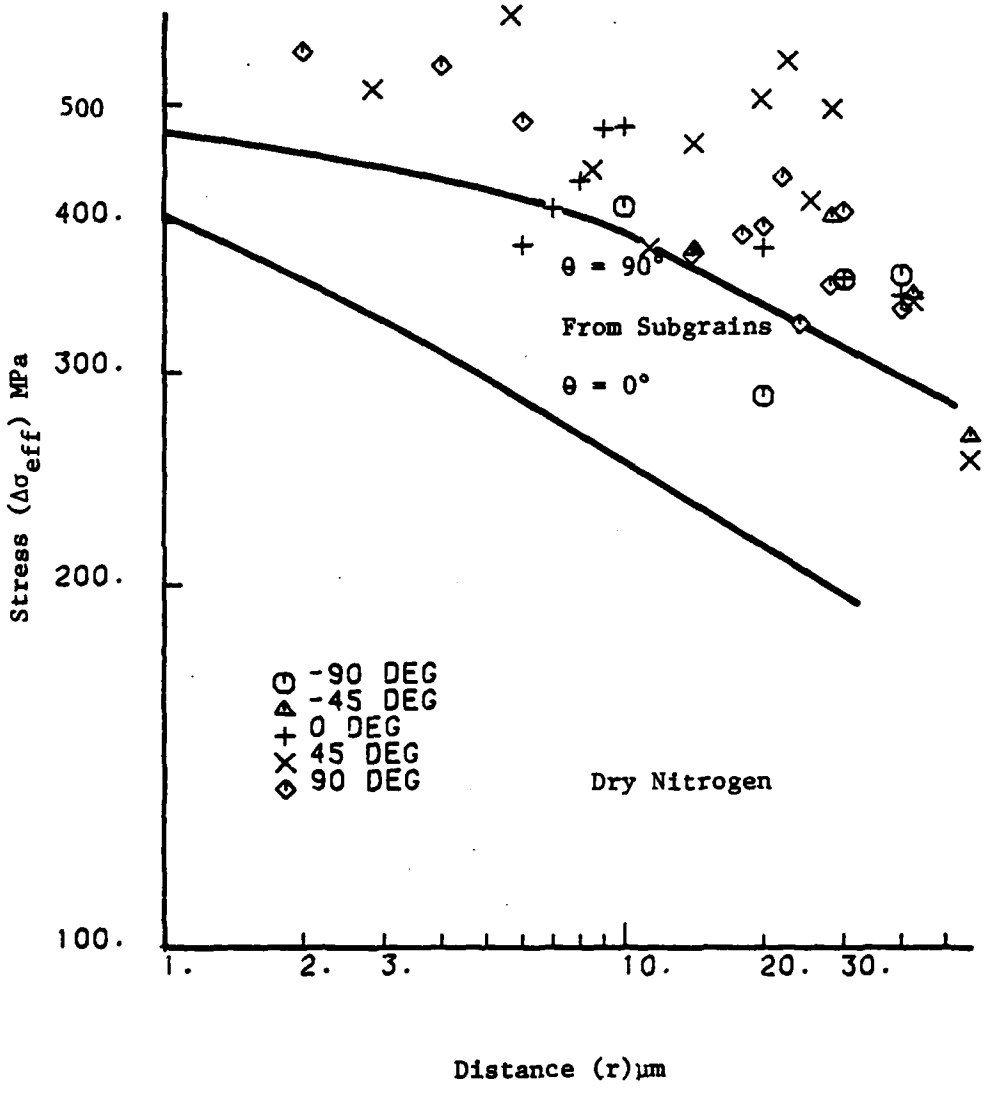

Figure 5. Effective stress vs. distance from crack tip for stress derived from subgrains and from stereoimaging.

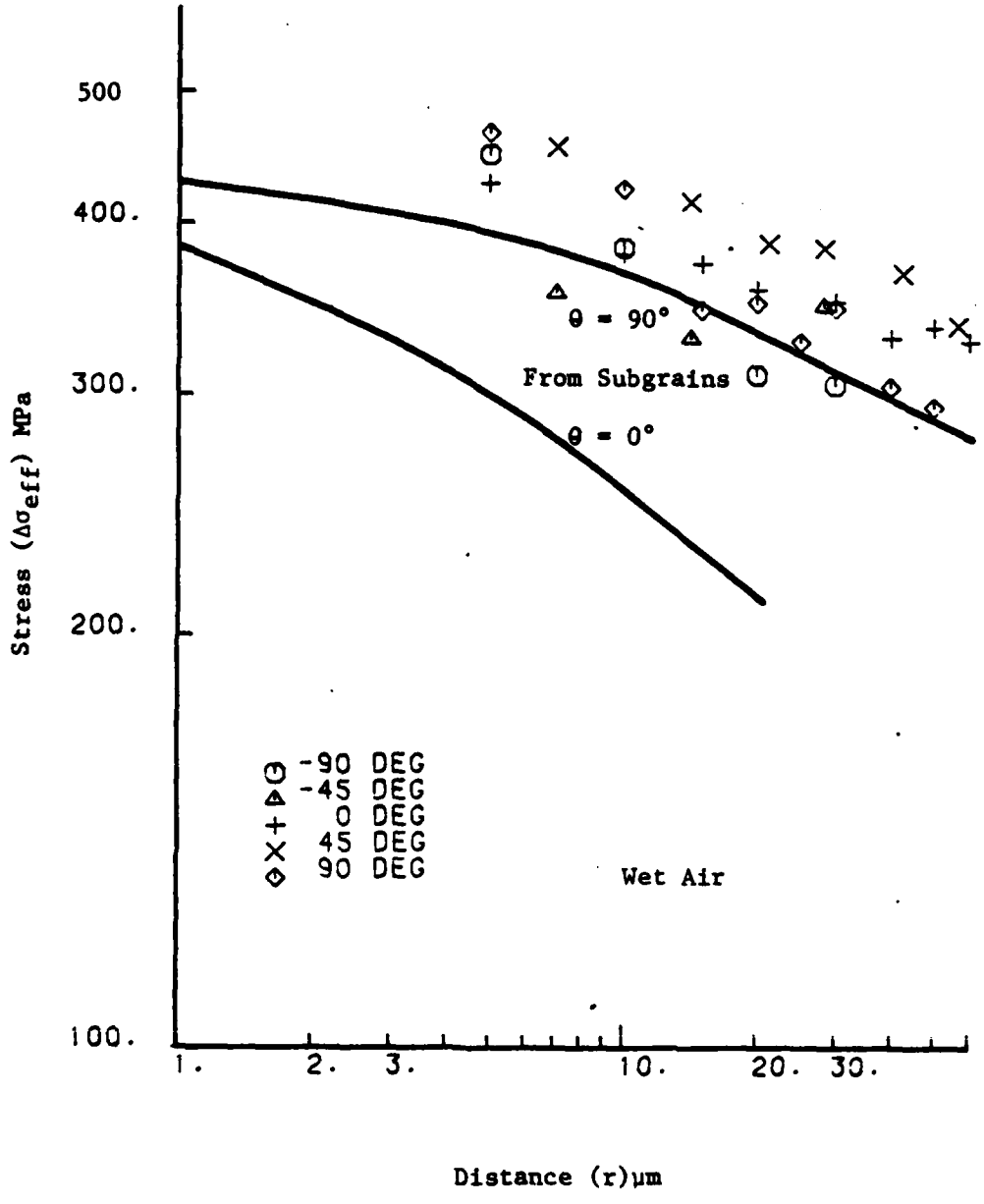

Figure 6. Effective stress vs. distance from crack tip for stress derived from subgrains and from stereoimaging.

Table 1

Environment	$\frac{\Delta\sigma}{\sigma_y}$ at crack tip: Subgrain Correlation	$\frac{\Delta\sigma}{\sigma_y}$ at crack tip: Computed from Strains
Dry Nitrogen	2.3	2.46
Wet Air	2.0	2.17
$\frac{\Delta\sigma_{wet}}{\Delta\sigma_{dry}} \mid r=0$	0.89	0.88

C. Calculation of Mean (or Hydrostatic) Stress Range

Calculation of mean stress range from the principal stress ranges is easily accomplished using the data of Figures 1 and 2 for the plane stress case. Figure 7 shows the computed mean stress ranges for the two environments directly ahead of the crack. The significance of the oscillations is not clear, and it is difficult to determine just what factors may be causing them because of the complex computational procedure used in their calculation. For the "plane strain" assumptions, the computational procedure is much simpler. Mean stress is computed directly from the average strain (see Appendix B); therefore, the average strain is also plotted on the figure. Mean stress as determined from average strain depends on the algebraic sum of $(\Delta\Gamma_1 + \Delta\Gamma_2)$, but since $\Delta\Gamma_2$ is nearly equal to the negative of $\Delta\Gamma_1$, it is the difference of two nearly equal numerical values which fixes the value of mean stress range. Thus, small errors in the determination of $\Delta\Gamma_i$ may be responsible for the oscillations observed. We have yet to resolve whether or not the oscillations are real or due to inaccuracies in determining of $\Delta\Gamma_1$ and $\Delta\Gamma_2$. At this time, it appears as though the magnitude of σ_m is relatively insigificant as a factor in environmentally assisted fatigue crack growth in this material except perhaps, very near ($r < 5$ μm) the crack tip.

In order to obtain σ_m, the maximum mean stress, calculated values of the mean stress range $\Delta\sigma_m$ must be added to σ_{min}. However, there is good reason to believe (see Section IV) that $\sigma_{min} << \Delta\sigma_m$, so that $\Delta\sigma_m \approx \sigma_m$.

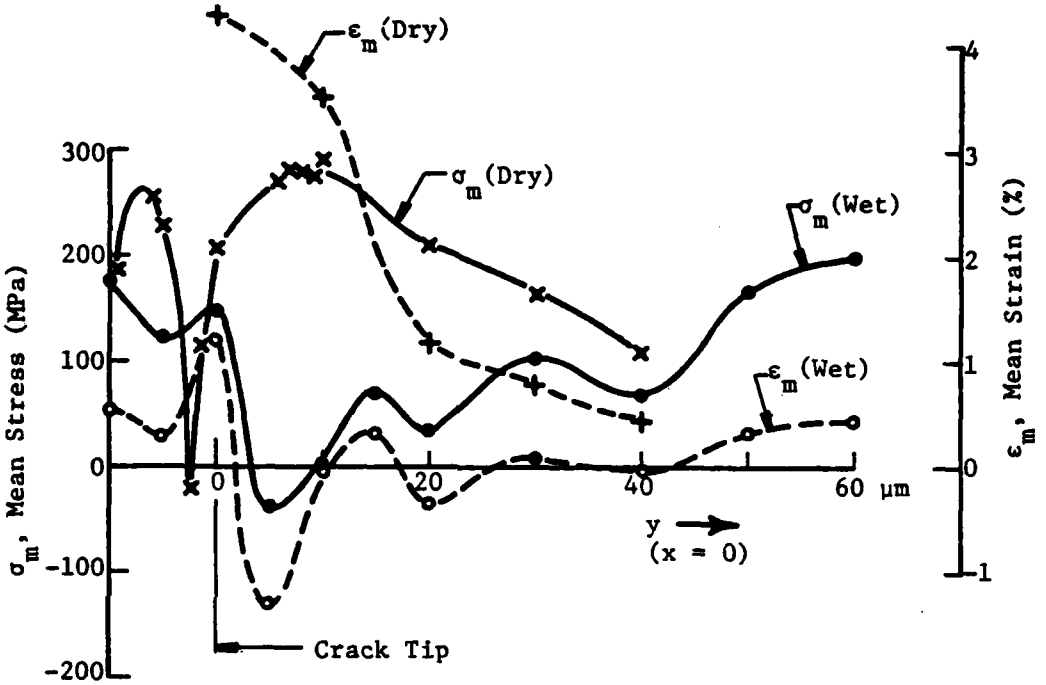

Figure 7. Mean stress and mean strain vs. distance ahead of crack for wet and dry environments.

III. CALCULATION OF THE ENERGY EXPENDED IN CREATING A UNIT AREA OF NEW CRACKED SURFACE

A computational procedure has been developed to make an estimate of the energy expended in creating new cracked surface from the data of a single load-unload pair of photographs of the crack tip. This section outlines the results of these computations and compares them to those previously obtained using subgrains[1] and strain gages[3] for strain and energy measurement. A more detailed account of the computational procedure and accompanying assumptions is given in Appendix C.

The energy computation begins with a knowledge of the effective strain increment $\Delta\varepsilon_{eff}$ at any point (x,y) within the crack tip plastic zone. This strain is computed through Eq. A8 in Appendix A, from the principal strains; these are computed from ε_x, ε_y and ε_{xy} as determined by stereoimaging analysis.

By plotting stress range vs. strain range for uncracked specimens, the cyclic stress-strain and hysteretic energy loss functions may be obtained. The work per cycle W_c is computed as the area within a hysteresis loop. Graphical representation of the results are given in Figure 8. The line through the data fits the equation

$$W_c = W_{co}' \Delta\varepsilon^m \tag{2}$$

where $W_{co}' = 675$ MJ/m^3 and $m = 1.14$.

An equation of the same form as (2) may be derived independently using subgrain data.[2] In this case correlation of the work per cycle with subgrain size gives

$$W_c = W_{co}\, d^{-1} \tag{3}$$

and correlation of $\Delta\varepsilon$ with subgrain size gives

$$\Delta\varepsilon = E_o d^{-m} \tag{4}$$

where $m = 0.84$. Combining (3) and (4) yields

$$W_c = W_{co} \left(\frac{\Delta\varepsilon}{E_o}\right)^{\frac{1}{m}} \tag{5}$$

where $\frac{1}{m} = 1.19$. Comparison of the exponential values shows very good agreement between the directly measured and derived values. Using $W_{co} = 3\times10^6$ J/m^3[1] and $E_o = .12$,[2] gives

$$W_c = 37.5\ \Delta\varepsilon^{1.19} \tag{6}$$

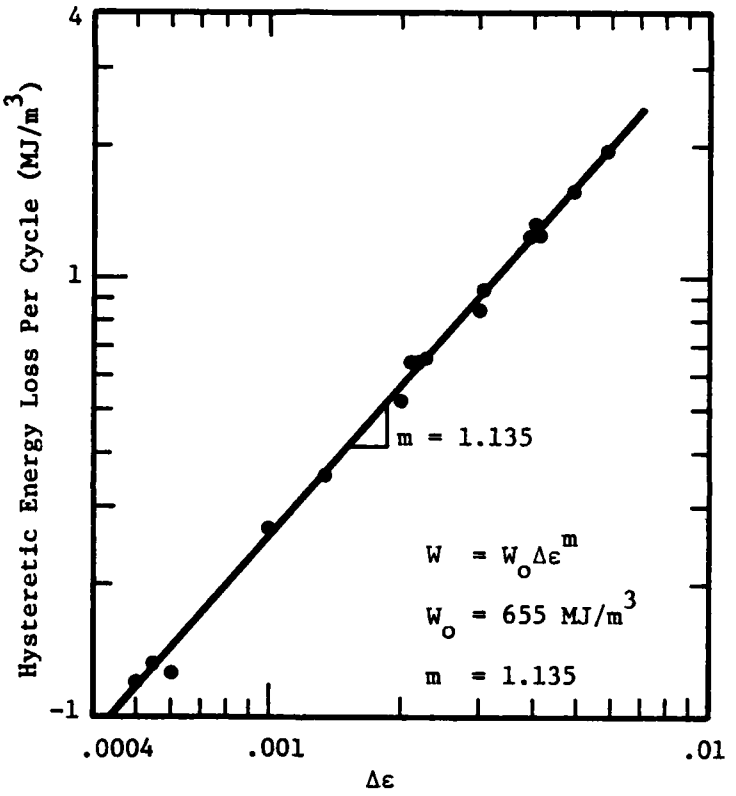

Figure 8. Hysteretic energy loss per cycle vs. strain range.

The pre-exponential factor as derived from subgrains is a factor of about 20 too small, but the exponent is in agreement. It is thus concluded that Eq. (2) has the correct functional form, and it is this relation which was used together with measured values of $\Delta\varepsilon_{eff}$ to compute the energy expended in creating new cracked surface, $^{dW}/_{dA}$.

For the stereoimaging strain data previously presented,[2] the computational results using Eq. (2) and the procedure of Appendix C are given in the following Table 2.

Table 2

Environment	ΔK $MN/m^{3/2}$	W_T MJ/m^2
Dry N_2	11	11.4
Wet Air	11	4.2
		7.2 = energy equivalent of the environment

These results are compared with those previously obtained by use of subgrains in Table 3, where an additional amount of energy of 3.6×10^6 J/m^2 has been added in order to account for energy dissipated outside of the subgrain forming region, as determined by Liaw, et al.[4]

Table 3

Environment	ΔK $MN/m^{3/2}$	W_T MJ/m^2
Dry N_2	11	4.7
Wet Air	11	3.9
		0.8 = energy equivalent of the environment

The magnitudes compare well for the wet air environment, and differ somewhat for the dry nitrogen environment, although the difference is not considered significant, considering the differences in the measuring techniques. The values as determined from subgrain and strain gage data are considered the more accurate because of the time-averaging of the data collection procedures for these calculations; the energy calculation from stereoimaging is only for one instance (cycle) and is not time averaged.

It is, therefore, only an estimate of the average value. The value of the computation is that it can be obtained very easily in the process of computing of strain and stress, and, at least in this case, gives a reasonable estimate of the energy magnitude, as compared with more laborious methods.

IV. STRAIN-RATE EFFECTS

In the 1979 Annual Report, displacement diagrams for the unloaded crack versus no crack were shown (Figs. 16 and 17). An analysis of this data revealed that compressive displacements, relative to the crack plane, existed in the crack tip region for the dry environment, and compressive displacements of about half this magnitude existed for the wet environment. In fact, these residual displacements were so large that full loading of the crack tip was insufficient to overcome them.

Further investigation of these observations has been made. The original observation concerned a crack tip loaded cyclically at 0.03 Hz. Subsequent investigation at 0.3, 0.1, 1.0, and 5 Hz has not indicated similar crack tip displacements, while duplication of the 0.03 Hz test showed findings which were qualitatively the same as previously reported. At the higher frequencies then, there is no (detectable) tensile or compressive residual displacement in the crack tip region, indicating that under such cyclic conditions, the crack tip strains are close to completely reversible.

The "compressive displacement" phenomena observed at 0.03 Hz is probably due to cyclic creep. Cyclic creep effects caused by tensile mean stress for plain carbon steel have been recently reported.[5] The low loading rate at 0.03 Hz is thought to give sufficient time for tensile creep near the crack tip to occur. When the crack is observed unloaded, the relative displacements of the crack flanks gives the appearance of compression on the crack plane, whereas actually the strains are tensile. These tensile strains are probably responsible for the development of compressive stresses due to the complete closure of the crack, but these have not actually been computed.

The lack of development of "compressive strains" at the crack tip for loading rates greater than 0.03 Hz, taken together with no abrupt change in the relation between crack growth rate and loading rate, indicates that this cyclic creep phenomenon is not of major significance in the lengthening of the fatigue crack, but, rather, this phenomenon is just another manifestation of the strain rate dependence of plastic deformation of low-carbon steel.

V. INTERPRETATION OF DATA

The information on crack tip plasticity which has been developed on this investigation to date is reviewed in this section and two interpretations of it are made. The first concerns the observations and measurements of the energy dissipated in advancing the fatigue crack and its variation with stress intensity factor and environment. Part A of this section is a reprint of a manuscript which was sent to, and has been tentatively accepted by, Fatigue of Engineering Materials and Structures.* Part B summarizes the findings of the investigation which are related to the detailed mechanistic understanding of crack propagation, and discusses the possible mechanisms of crack propagation which are compatible with these results.

---

*Figure numbers and references for this section are separate from those for the rest of the report.

A. INCORPORATING THRESHOLD AND ENVIRONMENTAL EFFECTS INTO THE DAMAGE ACCUMULATION MODEL FOR FATIGUE CRACK GROWTH

ABSTRACT

Measurement of the energy expended during growth of a fatigue crack in the near threshold region and how it is affected by a water vapor environment is coupled with direct observation of the crack tip to produce a modification of the damage accumulation model for fatigue crack growth which incorporates threshold and environmental effects.

INTRODUCTION

Although a large number of equations exist for calculating the growth rate of a fatigue crack, there is no general agreement as to which formulation approach is the most appropriate. This situation is at least partly true because of the very large number of variables to be considered in any experimental or applications situation. Several good recent catalogues of the different analytical approaches and the crack growth equations which result from them have been given.[1,2] Of these approaches, the crack growth models (as opposed to semi-empirical formulations) fall into essentially two categories:

1) Those based on a characteristic crack tip opening displacement (CTOD) criteria, which lead to the general relationship $\frac{da}{dN} \propto \Delta K^2$

2) Those based on a strain accumulation or damage criteria, which lead to the relationship $\frac{da}{dN} \propto \Delta K^4$

where da/dN is the crack growth rate, and ΔK is the cyclic stress intensity factor.

An excellent review of the details of derivation of the models fitting into these categories is given by Irving and McCartney.[3] These authors point out that values of the exponent of ΔK have been

measured between 2.3 to 19, but that most reliable data taken in an inert environment give a value of 4 ± 0.5.

A number of strain/damage accumulation models have been proposed. Weertman[3] seems to be the first to have formulated such a model, followed shortly thereafter by Rice. The theoretical concept was then further developed by Weertman[4] and Mura & Lin,[5] giving the general relation for crack growth rate as:

$$\frac{da}{dN} = \frac{(\Delta K)^4}{\mu \sigma^2 \gamma} F \qquad (1)$$

where μ = shear modulus, σ_y = an appropriate measure of strength, F = a geometric factor, and γ = the mechanical work input required for creation of a unit area of new crack surface. Another way of describing γ would be as the effective surface energy. Raju[6] has shown that Eq. (1) is a special case of the generalized relation he derived using an energy balance criteria for fracture.

It should be noted that Eq. (1) was derived for steady-state crack growth with the value of ΔK constant or ever increasing and with the linear, or Stage II, portion of the crack growth (da/dN vs ΔK) curve, and without consideration of any environmental effect. Irving and McCartney[2] have further refined Eq. (1) to account for the non-linear region of da/dN vs ΔK as $K \rightarrow K_{IC}$ (the fracture toughness stress intensity), and to account for the effects of changing R (K_{min}/K_{max}). Very recently Chakrabortty[7] has formulated a model which relates Stage II fatigue crack growth to low cycle fatigue properties, omitting the effects of environment, and including the threshold region only circumspectly.

The purpose of this paper is to show how Eq. (1) may be interpreted in the region of low ΔK, as $\Delta K \rightarrow \Delta K_{TH}$ (the threshold value of cyclic stress intensity), and how the effects of environment may be included in this description of fatigue crack propagation.

MEASUREMENT OF THE SURFACE ENERGY

A considerable body of experimental data for numerous materials exists to support a relation like that of Eq. (1), so it is considered as valid for steady-state growth, but the definitions of σ, F and γ all require some interpretation. The appropriate definition of σ is probably a "cyclic yield stress" or something akin to it, and F is probably best described (in practical terms) as a factor for correlating experimental data.

The work required for creation of a unit area of crack, γ, has been measured for several steels and aluminum alloys by a number of workers at Northwestern University; see the recent work of Fine[8] for a compendium of results. These measurements utilize a strain gage technique, which measures work absorption by the specimen as the fatigue crack lengthens. Due to the size of the strain gages, these measurements cannot be made within 200 μm of the crack plane.

Davidson & Lankford[9] have made similar measurements on low-carbon steel using electron channeling contrast to observe the subgrain forming region near the crack tip. A comparison of the two techniques by Liaw, Fine & Davidson[10] determined that the extrapolation technique within 200 μm of the crack tip, used in applying the strain gage method, was in agreement with the measurements made in that region by electron channeling,

and that the values of γ derived by channeling were too low (by about a factor of 2) because considerable hysteretic loss occurs in the specimen outside of the subgrain forming region.

The effect of environment on the magnitude of γ has been determined experimentally by Davidson & Lankford[9,11] to be ΔK dependent in the near threshold region, both for inert and water vapor environments, Fig. 1. The crack growth behavior observed fits the definition of "true corrosion fatigue" as defined by McEvily and Wei,[12] and Austen and Walker.[13] The data in Fig. 1, together with other experimental observations, will now be examined and a model presented for explaining the observed results.

A MODEL FOR THE NEAR-THRESHOLD REGION

The observed energy required for crack propagation, shown in Fig. 1, gives a value of γ for Eq. (1) that is constant in the limit (at higher ΔK). The ΔK corresponding to this limiting value of γ constitutes the lower limit of fully developed Stage II crack propagation. Most of the region shown in Fig. 1 covers that part of the crack growth curve where the threshold ΔK for crack propagation is being approached.

The crack tip region in this low-carbon steel has been observed in the scanning electron microscope (SEM) using a cyclic loading stage,[14] both after fatigue crack propagation in vacuum and in a 100% relative humidity environment. Although the SEM requires a vacuum for operation, there is a residual effect of environment which may last up to a hundred cycles. Thus, high resolution photographs of the crack tip region may be made for both environments in the SEM. Data are then derived from these photographs by the stereoimaging technique,[15] which allows displacements

of material in the plastic zone to be both seen and measured, as well as values of CTOD and opening load to be measured. The displacements may also be used to obtain five of the nine elements of the non-symmetric strain tensor.[16]

Use of these techniques has shown that the environment affects the mode of crack tip opening, the CTOD, the opening load, and the magnitude and distribution of strains in the plastic zone.[17] Changes in stress intensity are also observed to affect the opening mode.

The model being proposed here links these mode change observations with the energy measurements given in Fig. 1. The low ΔK region is expanded in Fig. 2, and the trends are extrapolated to encompass the threshold part of the crack propagation curve, and to show the elements of the model. The first observation is that a limiting value of γ is reached for ΔK in the region where Eq. (1) would be expected to be applicable (and for which it was derived).

For the dry nitrogen environment, the curve then develops a "U" shape as ΔK is decreased. The higher ΔK portion of the "U" is a transition region where the mode of crack opening is changing from predominantly Mode I. The lower ΔK region is postulated to exhibit a mode of crack opening which is dominated by Mode II. Since the crack is driven forward mainly by Mode I opening, the rate of crack growth in this region is decreasing; i.e., the exponent for ΔK (as in the Paris equation $\frac{da}{dN} = C\Delta K^m$) is becoming greater than 4. As the degree of Mode I decreases, the crack is beginning to wander through the material, creating a very rough fracture surface. Microscopically, this motion of the crack on planes not perpendicular to the load axis results in an increasing component of Mode II opening as ΔK decreases. In the limit, with decreasing ΔK, an

ever increasing input of mechanical energy to the specimen is required for each unit area of crack created, which is the definition of a threshold stress intensity factor. This near threshold region can be viewed in another way: since Mode II dominates the response of the crack to loading, the volume of material absorbing energy is small* and concentrated approximately along the plane of crack propagation; the crack is essentially made up of short sections of cracks growing in Stage I, a condition noted by numerous other investigators. As ΔK is increased, it is increasingly difficult to maintain this growth mode, and finally a transition to Stage II begins. The details of this transition depend upon a number of factors: surely the magnitude of $R = {}^{K_{min}}/_{K_{max}}$ and grain size will be important, as perhaps are several other metallurgical variables. The postulated effect of increasing R is shown on Fig. 2, and it is imagined that decreasing the grain size should have a similar effect. Some experimental verification of the grain size and R effects exists,[18] although detailed analysis of these experimental findings indicates considerable uncertainty in their interpretation.

The above discussion has been directed at the case of crack growth in an inert environment. For water vapor, an aggressive environment, the mechanism change on going from the fully Stage II region (limit) down to the ΔK threshold will essentially be the same, except that there is an equivalent input of energy by the environment which is ΔK dependent. The

---

* Actually the whole specimen is absorbing energy, hysteretically, in very small amounts per cycle. At the crack tip a relatively larger amount of energy is absorbed each cycle, and it is this energy to which this statement refers.

transition region between Mode I dominated crack growth and Mode II dominated growth will be lowered, as postulated on Fig. 2. It must be emphasized that in a water vapor environment for the region ΔK = 8 to 12 $MN/m^{3/2}$, experimental observation[17] has shown that Mode I is the predominant opening mode, and crack wandering is largely suppressed. A departure from this condition is beginning at ΔK = 10 $MN/m^{3/2}$, so that below ΔK = 4-6 $MN/m^{3/2}$ crack propagation might be expected to be classified as Stage I. The effect of increasing R would again be, as in the case for an inert environment, to extend to lower values of ΔK the transition to Stage I type growth. Since the mechanically input work for growing a crack in the water vapor environment is less, for a given ΔK, than in the inert environment, crack propagation rate should be greater, as is experimentally observed, and the $\Delta K_{Threshold}$ should be lowered for the water vapor environment, as experimentally observed.[12]* Equation (1) may be used to incorporate these observed changes through the modification of γ.

As derived, Eq. (1) incorporates γ as a term which is related solely to the amount of energy which was absorbed by the body as the crack was being lengthened. If the equivalent energy which is supplied by the environment, designated γ_e, is subtracted from γ then the effective energy $\gamma-\gamma_e$ causes the crack to advance faster for a fixed ΔK. No method has yet been devised for independently measuring γ_e.

---

* Note: These extrapolations do not consider changes in the type of corrosion assisted fatigue,[12] as may occur in some materials under some conditions.[18]

The mechanism by which γ is altered by environment is not known, but in a high humidity environment at low $\Delta K(<10\ MN/m^{3/2})$, flat facets appear on the fracture surfaces.[11,18] It is likely that these facets are indicative of intergranular fracture. However, near $\Delta K_{Threshold}$ fracture facets cease to appear.[18] These observations taken together with the decreased crack tip strain caused by a water vapor environment[17] are consistent with a lowering of γ.

Incorporating the effects of microstructure on the Mode I/Mode II mix of crack tip opening into Equation (1) is a more complex process, and one for which few guidelines exist. The lower the stacking fault energy (SFE), the higher the ΔK which might be expected to be predominated by Mode II, thus γ could be expected to increase with increasing SFE. Decreasing the grain size (when this is a relevant parameter) could reasonably be expected to have about the same effect as increasing R, and the evidence, Fig. 3, shows this trend may be correct. The effect of other metallurgical factors on γ, such as precipitate and dispersoid spacing, texturing, etc., is not known.

DISCUSSION

The theoretically derived equation for crack growth, Eq. (1), has been shown to have validity, at least for some materials and conditions, when steady-state Stage II fatigue crack propagation conditions are applicable. Irving and McCartney[2] have modified the equation to accommodate the high ΔK region where $K \rightarrow K_{IC}$, and Fine[8] has suggested that γ is dependent on ΔK, thereby accommodating those materials where the exponent of $\Delta K < 4$. The data of Figure 1 makes it possible to modify

Eq. (1) for the condition where $\Delta K \rightarrow \Delta K_{Threshold}$. The basis for Equation 1 to provide a framework for rationalizing fatigue crack growth in numerous alloy systems seems to be established, at least on a conceptual basis. Unfortunately it is difficult to measure γ, and it needs to be determined for a larger number of alloy systems under known conditions before knowing the breadth of applicability of this framework.

Likewise a direct method for measurement of $\gamma_{environment}$ is not available, and it has been measured indirectly only for low-carbon steel. To make this situation more complex, the crack opening mode is changing in the near-threshold region, and this interacts with both the environment and the microstructure of the material. Because of these complex interactions which will change with alloy, microstructure and environment, it may be that an approach which reflects these complexities through γ provides the best overall description of the threshold phenomenon. There is also hope that γ will become easier to measure for a broader range of materials and environments as methods are devised to use the strain information derived by the stereoimaging method for calculating the work required for the creation of new fracture surface.

CONCLUSIONS

1) The effect of decreasing stress intensity factor magnitude on the mechanical work expended in forming a unit area of new fatigue crack surface may be explained by changes in the predominant mode of crack opening from Mode I to Mode II.

2) The value of $\Delta K_{Threshold}$ may be defined by postulating that at very low values of ΔK, the change to Mode II is nearly complete and that the magnitude of loading is so small that the large amount of work which must be put into the specimen results in a vanishingly small crack growth.

3) The effect of environment, for a decreasing ΔK, is to move the transition of crack opening mode from Mode I to Mode II down to lower values of ΔK.

4) When the above observations are brought together and expressed in the form of the energy required to make a unit area of new cracked surface, they fit conveniently into the crack growth rate equation originally formulated by Weertman[3] for Stage II fatigue crack propagation. With the modification of Irving and McCartney for the high ΔK region this type of equation may be used over the full range of crack growth rates as a framework for calculating steady-state fatigue crack growth.

5) The expected effect of changing R ratio is shown in Fig. 2, but the change in $\Delta K_{Threshold}$ with changes in both R ratio and grain size is likely to be very complex.[18]

ACKNOWLEDGEMENT

This concept was discussed with numerous persons as it was being formulated, and their questions and insights were very helpful; discussions with the following individuals is specifically acknowledged: Dr. S. G. Druce, Dr. J. Lankford, Dr. J. Schijve and Dr. B. Tomkins. Financial support of The Office of Naval Research, Contract N 00014-75-C-1038 is gratefully acknowledged.

REFERENCES

(1) Chakrabarti, A. K. (1978) Eng. Frac. Mechanics 10, pp. 469-483.

(2) Irving, P. E., and McCartney, L. N. (1977) Metal Science 11, pp. 351-361.

(3) Weertman, J. (1966) Int. J. Fracture Mech. 2, p. 460.

(4) Weertman, J. (1973) Int. J. Fracture Mech. 9, p. 125.

(5) Mura, T. and Lin, C. T. (1974) Int. J. Fracture Mech. 10, p. 284.

(6) Raju, K. N. (1972) Int. J. Fracture Mech. 8, pp. 1-14.

(7) Chakrabortty, S. B. (1979) Fatigue of Eng. Mat. Struct. 2, p. 331.

(8) Fine, M. E. (1980) Met. Trans. 11A, p. 365.

(9) Davidson, D. L. and Lankford, J. (1979) "Environmental-Sensitive Fracture of Engineering Materials," ed. Z. A. Foroulis, AIME, pp. 581-594.

(10) Liaw, P., Fine, M. E. and Davidson, D. L. (1980) Fatigue of Eng. Mater. and Struc. 2 (in press).

(11) Davidson, D. L. and Lankford, J. (May 1978) Report to The Office of Naval Research on "Crack Tip Plasticity Associated with Corrosion Assisted Fatigue," Contract N 00014-75-C-1038.

(12) McEvily, A. J. and Wei, R. P. (1972) in "Corrosion Fatigue: Chemistry, Mechanics, and Microstructure," NACE 2, Houston, pp. 381-395.

(13) Austen, I. M. and Walker, E. F. (1977) in "The Influence of Environment on Fatigue," I. Mech. E, London, pp. 1-10.

(14) Davidson, D. L. and Nagy, A. (1978) J. of Phys. E 11, pp. 207-210.

(15) Davidson, D. L. (1979) SEM/1979/II, SEM, Inc., AMF O'Hare, IL, pp. 79-86.

(16) Williams, D. R., Davidson, D. L. and Lankford, J. (1980) Exper. Mechanics 20 (in press).

(17) Davidson, D. L. and Lankford, J. (May 1979) Report to the Office of Naval Research on "Crack Tip Plasticity Associated with Corrosion Fatigue," Contract N 00014-75-C-1038.

(18) Druce, S. G. (1977) "Fatigue of Ferritic Steels," Ph.D. Thesis, University of Birmingham, UK, Fig. 92.

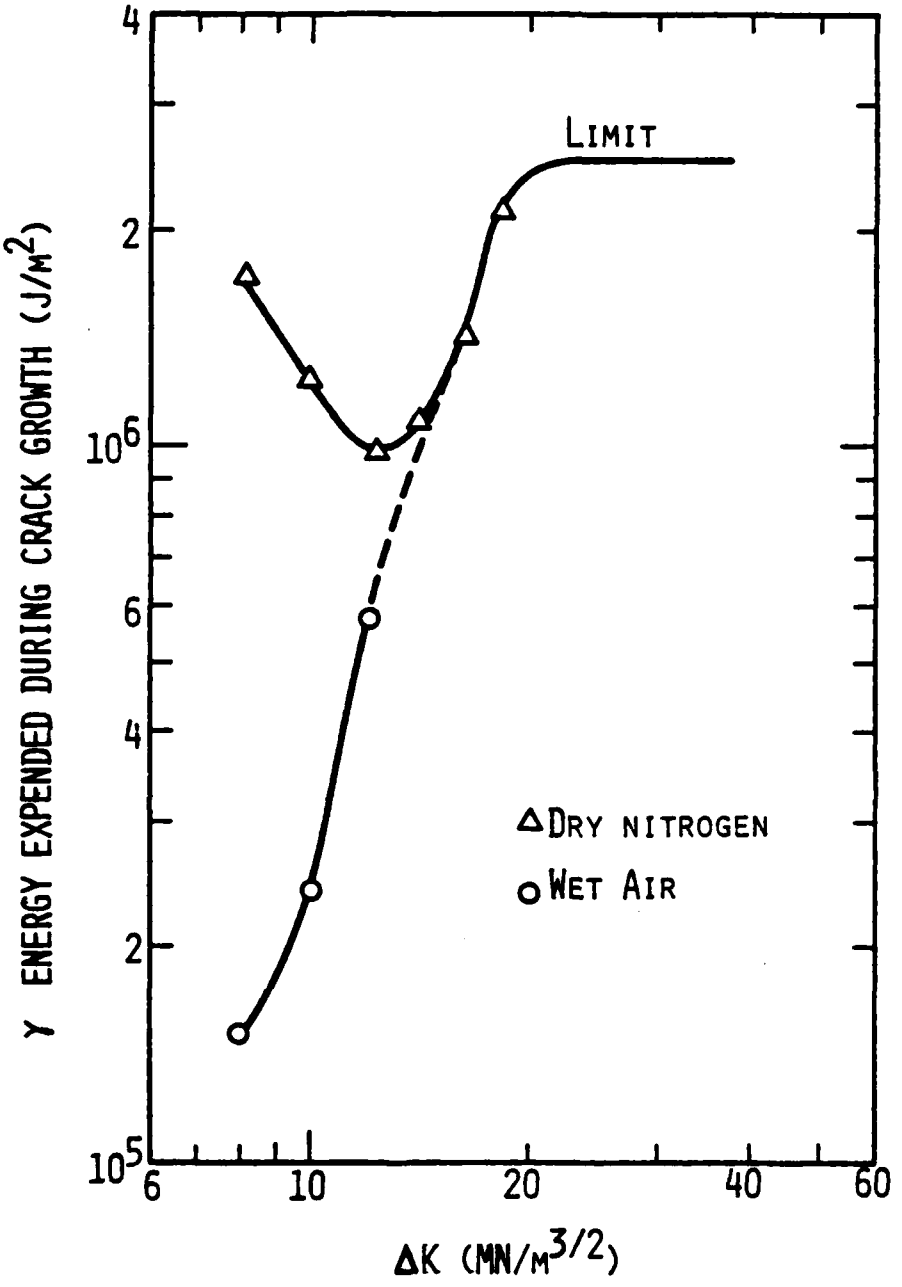

Figure 1. Energy expended to grow a fatigue crack as a function of cyclic stress intensity showing the effect of environment.

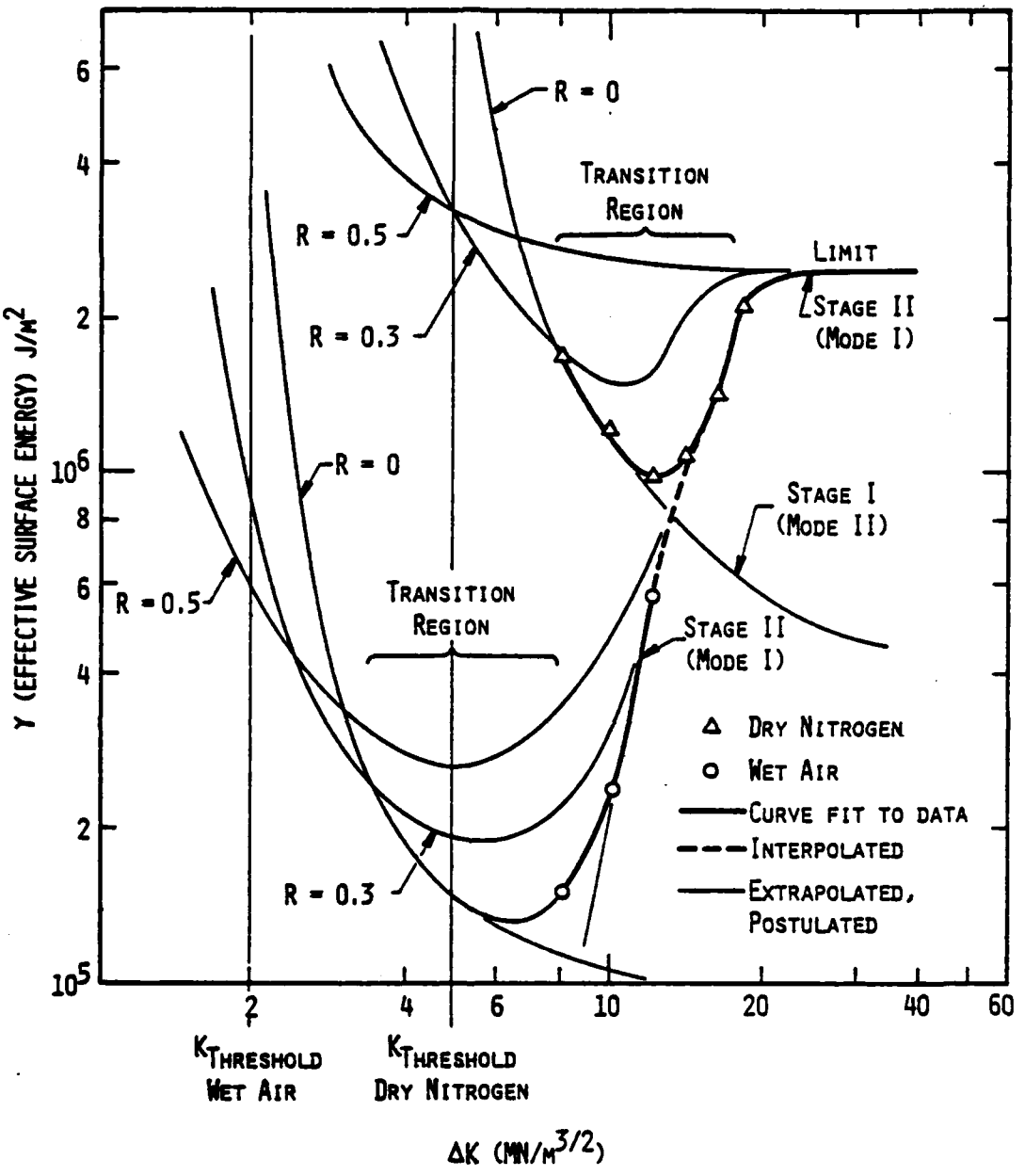

Figure 2. Extrapolation and interpretation of the data shown in Figure 1.

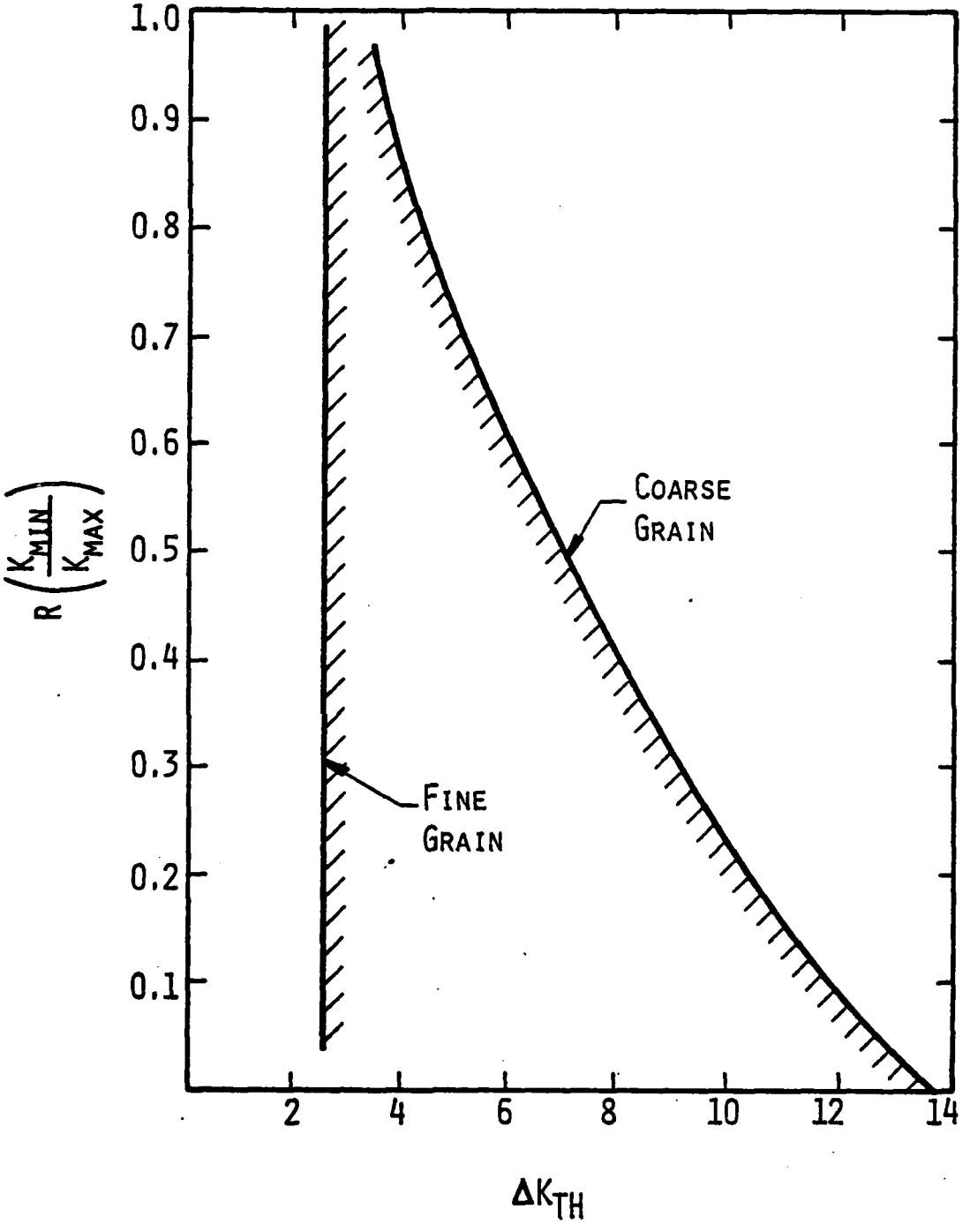

Figure 3. The effect of grain size and R ratio on threshold ΔK for 16 different steels tested in air. The lines describe the bounds for the correlation, which includes 102 data points. After S. G. Druce.[18]

B. Summary and Interpretation of Information Related to the Mechanism of Environmentally Assisted Fatigue Crack Propagation

To date, experimental observations have determined that the effects of a water vapor environment on crack tip plasticity parameters for low-carbon steel are as follows:

1) The energy dissipated in forming new crack surface is lowered, and is ΔK dependent in the near threshold region.

2) The stress range magnitude is lowered, and is ΔK dependent.

3) The strain range magnitude is lowered.

4) The size of the subgrain forming region, which is proportional to the plastic zone size, is decreased, and is ΔK dependent.

5) The mix of deformation modes is changed to more Mode I (less Mode II).

6) On the fracture surface, "brittle," probably intergranular facets, begin to appear as ΔK is decreased.

From these observed changes, it is clear that both the magnitude and spatial extent of crack tip plasticity are reduced by a water vapor environment as ΔK_{th} is approached. But, what do these findings imply about the material property changes in the element which will be fractured, thereby advancing the crack, on the next tensile portion of the loading cycle? And, exactly where are the material properties affected by the environment--it seems clear enough that they are affected just adjacent to the crack tip, but are they also affected farther out in the plastic zone?

The only atomic species available at the crack tip in a water vapor environment are hydrogen and oxygen. From the work of Dwyer, Simmons and Wei,[6] there seems to be little doubt that hydrogen is the element responsible for whatever changes are found. Hydrogen could alter material properties in one or more of four ways. It could:

1) increase or decrease the flow stress;

2) increase or decrease the strain to fracture;

3) change the work-hardening characteristics; and

4) lower the surface energy at the crack tip.

For material properties to be altered beyond the immediate crack tip region, farther out into the plastic zone, transport of the hydrogen into that region would be required. This movement of the hydrogen could,

conceptually, be accomplished by concentration gradient and stress gradient driven diffusion and by dislocation sweep in.

First, the possible material property changes immediately adjacent to the crack tip will be examined:

1) Since the energy dissipated in forming the crack is lowered, the area beneath the stress-strain curve must be decreased.

2) Since the crack tip strain magnitude is decreased by about a factor of 2, this must be a major contributor to the decrease in energy dissipation (and area beneath the stress-strain curve).

3) The decrease in stress magnitude determined both from subgrain size and from strains by stereo-imaging assumes no change in the stress-subgrain or stress-strain relations for hydrogen charged material. If this assumption was not correct, then, effectively, the correlation between stress range and subgrain size would have to be thought of as being altered by the presence of hydrogen. Indeed, it is possible to make the assumption that the stress range at the crack tip is not altered by environment, and back calculate the functional relation between stress range and subgrain size. But since the alteration of stress range at the crack tip is ΔK dependent,[1] this would mean that a different correlation between stress range and subgrain size would be required for each ΔK, and this is not physically plausible. Thus, the decrease in the stress range in a wet environment appears to be a real effect, and must be explained by either a change in yield stress or work hardening or both. If the water vapor environment is not to alter the ratio of stress range/yield stress, then the effect of hydrogen must be to decrease the yield stress, which is not likely for low-carbon steel[7,8] (although it might be for pure iron). A decrease in yield stress should cause a larger plastic zone, but a smaller plastic zone is actually observed, indicating that the yield stress ought to be increasing. If yield stress increases, then this would cause the stress range/yield stress ratio to be further lowered.

4) The possibility of a change in work hardening coefficient may also be considered by examining the stress and strain distributions. A change in work hardening would be manifested in a change in

stress and strain distribution functions in the way outlined by Rice and Rosengren,[9] who found $\sigma \propto r^{\frac{N}{1+N}}$ and $\varepsilon \propto r^{\frac{1}{1+N}}$. Previously,[1] the stress distribution was found to be $\sigma \propto r^{-.26}$; this value came from the correlation of stress range and subgrain size. From this, a strain distribution $\varepsilon \propto r^{-.82}$ was derived; it was possible to obtain a check on the validity of this by stereoimaging.[2] These distribution functions would result if N = 0.31, which is about the value obtained by Landgraf[10] for low-carbon steel. The effect of water vapor is to change the magnitudes of these functions at the crack tip, but <u>not the distribution</u> function (slope). It is therefore concluded that work hardening of the material is not changed substantially by the presence of hydrogen.

5) To examine the possibility that hydrogen lowers the surface energy at the crack tip and that this is the relevant material alteration, it is useful to compare the magnitudes of the energy dissipated in lengthening the crack versus the surface energy, Table 4.[2]

Table 4

Condition	Energy (J/m^2)	$\Delta K(MN/m^{3/2})$
No Environmental Effect	17.1×10^5	8
With Environment	1.5×10^5	8
Surface Energy	2	

Thus, the environmental effect is in the range of 15.6×10^5 J/m^2 as compared to 2 J/m^2 for the surface energy. If, for example, the environment were to lower the surface energy to 1 J/m^2, no model exists which can explain how this might have a 1×10^6 J/m^2 effect on the energy dissipated in forming new crack. This possibility, therefore, is excluded.

The above analysis argues for the fact that hydrogen alters only one material property in a substantial way; the strain to fracture is decreased by about a factor of 2. The yield and flow stress may, or may not, be altered, but if there is any change, it is not very large; not over $\pm$ 15%.

The conclusion that work hardening is not changed could also be interpreted as follows: since the distribution functions of stress and strain are not substantially altered, but the magnitude (coefficient) of the function is, this is indicative of only a small volume of the material immediately at the crack tip which has been affected by the hydrogen, rather than a substantial portion of plastic zone. If correct, then, this finding could mean that the effect of hydrogen was simply "embrittlement," and would obviate the requirement for hydrogen to be transported into the material to any great distance by either diffusion or dislocation sweep-in.

VI. SUMMARY AND CONCLUSIONS

1. A computational procedure for calculating stress from strain, (as determined by stereoimaging) has been found, and stresses in the crack tip plastic zone have been computed.

2. The magnitude of the crack tip stresses calculated from measured strains agrees reasonably well with those determined previously using subgrains, as detected by electron channeling. The distribution of stress along some radial directions, however, differs between the two methods.

3. The strains determined by stereoimaging have also been used to calculate the energy dissipated in forming new crack surface, and the results agree reasonably well with those obtained from subgrain size distribution, as previously determined.

4. Previously reported crack tip "clamping displacements" have been further investigated and found to be loading rate dependent. As such, they are thought to be a cyclic creep effect, and not directly related to fatigue crack propagation.

5. The previously determined changes of energy dissipation to form new crack surface with environment and ΔK have been incorporated into the damage accumulation model for fatigue crack growth and a manuscript prepared for publication.

6. The crack tip plasticity data which has been collected to date is summarized, and analysed to determine the effect of the environment on material properties in the crack tip region. Hydrogen is considered to be the dominant environmental specie. It is concluded, based on the available evidence, that the major effect of hydrogen is to reduce the strain to fracture in the region just adjacent to the crack tip, and that the material properties farther out in the plastic zone are not greatly affected.

VII. REFERENCES

1. D. L. Davidson and J. Lankford, Office of Naval Research Annual Report, 1978, available from NTIS, Port Royal, Virginia, and the authors.

2. D. L. Davidson and J. Lankford, Office of Naval Research Annual Report, 1979.

3. S. Ikeda, Y. Izumi and M. E. Fine, Eng. Fract. Mech. 9, 123 (1977).

4. P. K. Liaw, M. E. Fine and D. L. Davidson, Fatigue of Eng. Materials and Struct., in press (1980).

5. D. Pilo, W. Reik, P. Mayr and E. Macherauch, ibid, 1, 287 (1979).

6. D. J. Dwyer, G. W. Simmons and R. P. Wei, Surface Science 64, 617 (1977).

7. S. Asano and R. Otsuka, Scripta Met. 10, 1015-1020 (1976).

8. H. Kimura, H. Matsui and S. Moriya, Scripta Met. 11, 473 (1977).

9. J. R. Rice and G. F. Rosengren, J. Mech. Phys. Solids 16, 1 (1968).

10. R. W. Langraf, "Work Hardening in Tension and Fatigue," AIME, New York, 1977, p. 240.

APPENDIX A

CALCULATION OF STRESS

Calculation of the principal stress ranges from the principal strain ranges has been done according to the method given by Lubahn and Felgar.[1] The authors are endebted to Prof. S. R. Bodner of the Technion for pointing out this and other references to them.

In order to make the calculation, it is necessary to make a number of assumptions:

1) Plane stress, $\sigma_3 = 0$.

2) $\Gamma_i = \varepsilon_i + e_i$; ε_i = plastic strain, e_i = elastic strain (A1)

3) The deformation theory of plasticity pertains, so that, with $\sigma_3 = 0$,

$$\frac{\varepsilon_1 - \varepsilon_2}{\sigma_1 - \sigma_2} = \frac{\varepsilon_2 - \varepsilon_3}{\sigma_2} = \frac{\varepsilon_3 - \varepsilon_1}{-\sigma_1} \tag{A2}$$

4) During deformation, plastic strains do not change the volume, so that

$$\varepsilon_1 + \varepsilon_2 + \varepsilon_3 = 0 \tag{A3}$$

5) The elasticity relations are

$$\left.\begin{aligned} \varepsilon_1 &= \frac{\sigma_1}{E} - \frac{\mu}{E}\sigma_2 \\ \varepsilon_2 &= \frac{\sigma_2}{E} - \frac{\mu}{E}\sigma \\ \varepsilon_3 &= -\frac{\mu}{E}(\sigma_1 + \sigma_2) \end{aligned}\right\} \tag{A4}$$

where μ = Poisson's ratio and E = Young's Modulus.

These equations may be combined and reduced to the quadratic

$$a\sigma_2^2 + b\sigma_2 + c = 0 \tag{A5}$$

where $a = 1-2\mu$; $b = -E(2\Gamma_1 + \Gamma_2)$; $c = -[\sigma_1^2(1-2\mu) - E\sigma_1(2\Gamma_2 + \Gamma_1)]$

so that

$$\sigma_2 = \frac{-b-\sqrt{b^2 - 4ac}}{2a} \tag{A6}$$

Measured values are $\Delta\Gamma_i$, the principal strain ranges. It is assumed that the above equations can also be used to calculate $\Delta\sigma_i$.

The computational procedure for calculation of principal stress range is as follows:

1. Assume a value of $\Delta\sigma_1$.

2. Compute $\Delta\sigma_2$ from (A6).

3. Compute

$$\Delta\sigma_{eff}^{s} = (\Delta\sigma_1^2 - \Delta\sigma_1\Delta\sigma_2 + \Delta\sigma_2^2)^{1/2} \tag{A7}$$

4. Compute Δe_i from (A4).

5. Compute $\Delta\varepsilon_i$ from (A1).

6. Compute

$$\Delta\varepsilon_{eff} = \frac{2}{\sqrt{3}}(\Delta\varepsilon_1^2 + \Delta\varepsilon_1\Delta\varepsilon_2 + \Delta\varepsilon_2^2)^{1/2} \tag{A8}$$

7. Determine $\Delta\sigma_{eff}^{e}$ from the cyclic stress-strain curve*

$$\Delta\sigma_{eff}^{e} = K'(\frac{\Delta\varepsilon_{eff}}{2})^{m} \tag{A9}$$

8. Compare $\Delta\sigma_{eff}^{s}$ to $\Delta\sigma_{eff}^{e}$. If unequal, assume another value of $\Delta\sigma_1$ and iterate. A new value of $\Delta\sigma_1$ is determined from

$$\Delta\sigma_1' = \Delta\sigma_1(\frac{\Delta\sigma_{eff}^{e}}{\Delta\sigma_{eff}^{s}}) \tag{A10}$$

---

*Cyclic stress-strain curves are usually obtained from a specimen stressed along one axis, while the fatigue crack creates a biaxial stress state. It has been assumed that the cyclic stress-strain curve may be related to the multiaxial case through use of the effective stress and strain. This assumption has been examined by Lambda and Sidebottom,[2,3] who found no reason to invalidate, or greatly modify, it.

References
(Appendix A)

1. J. D. Lubahn and R. P. Felgar, "Plasticity and Creep of Metals," John Wiley and Sons, New York, 1961, pp. 321-339.

2. H. S. Lambda and O. M. Sidebottom, J. Eng. Mat. and Tech. (ASME) 100, 96-103 (1978).

3. H. S. Lambda and O. M. Sidebottom, ibid, p. 104 (1978).

APPENDIX B

COMPUTATION OF MEAN (HYDROSTATIC) STRESS RANGE

1. By definition $\Delta\sigma_m = \frac{1}{3}(\Delta\sigma_1 + \Delta\sigma_2)$; $\Delta\sigma_3 = 0$ (B1)

   where values of $\Delta\sigma_1$ and $\Delta\sigma_2$ are determined from the plane stress assumptions of Appendix A.

2. If a condition of plane (plastic) strain is assumed, so that $\Delta\varepsilon_3 = 0$, a value of the mean stress can be determined (but not σ_1 and σ_2 individually). $\Delta\sigma_1 + \Delta\sigma_2 = 2\Delta\sigma_3$.

$$\Delta\sigma_m^{A} = \Delta\sigma_3 = \frac{E}{(1-2\mu)}\left(\frac{\Delta\Gamma_1 + \Delta\Gamma_2}{2}\right) \tag{B2}$$

3. If a condition of plane (total) strain is assumed, so that $\Delta\Gamma_3 = 0$, $\Delta\varepsilon_3 = 0$, $\Delta e_3 = 0$, then

$$\Delta\sigma_1 + \Delta\sigma_2 = \frac{1}{\mu}\Delta\sigma_3$$

$$\Delta\sigma_m^{B} = 1.523\Delta\sigma_3$$

   where $\Delta\sigma_3$ is given by Eq. (B2).

   Determination of $\Delta\sigma_1$ and $\Delta\sigma_2$ may be intractable, an extended effort has not been made to obtain solutions for them.

4. If a condition of plane (total) strain is assumed, so that $\Delta\Gamma_3 = 0$ and $\Delta\varepsilon_3 = -\Delta e_3$, then

$$\Delta\sigma_m^{C} = \frac{E}{(1-2\mu)}\left(\frac{\Delta\Gamma_1 + \Delta\Gamma_2}{3}\right)$$

Table B1

Summary of Plane Strain Assumptions

Designation	Assumptions	Mean Stress
A	$\Delta\varepsilon_3 = 0$	$\Delta\sigma_m^{A} = \Delta\sigma_3 = \frac{E}{(1-2\mu)}\left(\frac{\Delta\Gamma_1 + \Delta\Gamma_2}{2}\right)$
B	$\Delta\Gamma_3 = 0$, $\Delta\varepsilon_3 = 0$, $\Delta e_3 = 0$	$1.523\Delta\sigma_3$
C	$\Delta\Gamma_3 = 0$, $\Delta\varepsilon_3 = -\Delta e_3$	$\frac{2}{3}\Delta\sigma_3$

Thus, the assumptions giving $\Delta\sigma_m{}^A$ lie between those yielding $\Delta\sigma_m{}^B$ and $\Delta\sigma_m{}^C$:

$$\Delta\sigma_m{}^C = \frac{2}{3}\Delta\sigma_m{}^A \qquad \Delta\sigma_m{}^B = \frac{3}{2}\Delta\sigma_m{}^A$$

All these plane strain assumptions depend on the quantity $(\Delta\Gamma_1 + \Delta\Gamma_2)$, but algebraically, since $\Delta\Gamma_2$ is negative, this becomes the numerical difference between the magnitudes of $\Delta\Gamma_1$ and $\Delta\Gamma_2$, which is usually a small quantity. The term $\frac{E}{1-2\mu} = 4.5\text{x}10^5$ MPa,* thus the actual value of $\Delta\sigma_m$ is extremely sensitive to small differences in $\Delta\Gamma_1$ and $\Delta\Gamma_2$. The mean strain range $(\frac{\Delta\Gamma_1 + \Delta\Gamma_2}{2})$ is shown as the number at each point in Figures 3 and 4. Magnitudes for the plane strain estimates of $\Delta\sigma_m$ given in Table B1 may be made using these mean strain values directly. A (typical) mean strain of 0.4%, therefore, gives $\Delta\sigma_m = 1800^{+1100}_{-600}$ MPa, all of which are believed to be unrealistically high.

Reference
(Appendix B)

1. A. Nadi, "Theory of Flow and Fracture of Solids," Volume II, McGraw Hill, New York, 1963, p. 30ff.

*Poisson's ratio was taken as $\mu = 0.28$; see Nadi[1] for more information.

APPENDIX C

THE ENERGY EXPENDED IN FORMING A UNIT AREA OF NEW CRACK SURFACE

This appendix outlines the method used in computing the energy expended in creating a unit area of new crack surface, W_T, using the strains computed by stereoimaging analysis.

1. In the reduction of data from a pair of photographs, one of the crack tip loaded, the other unloaded, the strain ranges $\Delta\varepsilon_x$, $\Delta\varepsilon_y$ and $\Delta\gamma_{xy}$ are determined at numerous points x, y within the plastic zone of the crack tip.

2. From these normal strain ranges the principal strain ranges are computed, using a Mohr's circle construct. An "effective strain range"[1] is then computed as

$$\Delta\varepsilon_{eff} = \frac{2}{\sqrt{3}}(\Delta\varepsilon_1^2 + \Delta\varepsilon_1\Delta\varepsilon_2 + \Delta\varepsilon_2^2)^{1/2} \qquad (C1)$$

3. The hysteretic energy loss per cycle is found to be

$$W_c = W_{co}'\Delta\varepsilon^m \qquad (C2)$$

Where $W_{co}' = 675$ MJ/m^3 and $m = 1.14$.

4. The computed value of $\Delta\varepsilon_{eff}$ is then put into (C2) and W_c is obtained for each x,y point. A point actually represents a small volume of material, defined by the x and y spacing of points on the surface as A(x,y), and one unit deep.

5. The total energy expended during that one loading of the crack tip is the sum of all the products, W_cA

$$W = \sum_{x,y} W_c(x,y)A(x,y) \qquad (J/m) \qquad (C3)$$

6. To obtain dW/dA, several assumptions are required:

   a. For a given value of x, the function $\Delta\varepsilon_{eff}(y)$ is typical of the strain history experienced by a small volume of material during the passage of the fatigue crack.

   b. The small volume of material Δx, Δy, Δz represented by each point x,y experiences a number of cycles ΔN, which is determined by $\Delta y/\frac{da}{dN}$.

c. The energy expended by each element x,y as the crack passes is $\Sigma_y \Delta N \, \Delta\varepsilon_{eff}(y)$.

7. With these assumptions: $dW/dA = \Sigma_x \Sigma_y \Delta N \, \Delta\varepsilon_{eff}(x,y)$. But, $\Sigma_y \Delta N = N$, where N = the number of cycles which caused the crack to advance a distance from the crack tip to the limit of the analysis (which is usually the edge of the photograph). Therefore, dW/dA becomes simply

$$dW/dA = \frac{W}{da/dN} \qquad (J/m^2) \qquad (C4)$$

where W is determined by Eq. (C3).

References
(Appendix C)

1. J. D. Lubahn and R. P. Felgar, "Plasticity and Creep of Metals," John Wiley and Sons, New York, 1961, pp. 285ff.